Engineering Structures 33 (2011) 2509–2524

Contents lists available at ScienceDirect

Engineering Structures

journal homepage: www.elsevier.com/locate/engstruct

Estimation of the Park–Ang damage index for planar multi-storey frames using equivalent single-degree systems

Siddhartha Ghosh [*,1], Debarati Datta [2], Abhinav A. Katakdhond [3]

Department of Civil Engineering, Indian Institute of Technology Bombay, Mumbai 400076, India

ARTICLE INFO

Article history:
Received 13 October 2010
Received in revised form
13 April 2011
Accepted 26 April 2011
Available online 1 June 2011

Keywords:
Park–Ang damage index
Equivalent systems
Modal pushover analysis
Performance-based evaluation
Performance-based design

ABSTRACT

A detailed characterization of potential structural damage is essential to performance-based seismic design. The Park–Ang damage index is selected in this work as the seismic damage measure, since it is one of the most realistic measures of structural damage. Response spectra constitute the most common tool used for characterizing the seismic hazard at a site, and these spectra represent the demand on single-degree oscillators. To use these spectra for estimating the Park–Ang damage index demand on an MDOF system, three equivalent single-degree system-based approximate schemes are proposed. These schemes are tested on three moment resisting frames under several ground motion scenarios. The effectiveness of an equivalent system scheme is measured by comparing with the estimates from a nonlinear response-history analysis of the MDOF model. These schemes are tested for both global and storey-level damage indices. Variation of the non-dimensional parameter β is also considered in these case studies. Overall, all the three schemes are found to be effective with varying degrees of accuracy. The proposed methods are recommended for damage-based seismic design and performance evaluation of structures because these schemes can use response spectra for demand estimation and reduce computation cost.

1. Performance-based seismic design

For over more than a decade now, performance-based seismic design (PBSD) has been at the forefront of earthquake engineering research. One of the prime aspects of PBSD is the realistic characterization of seismic structural damage and its direct incorporation in the design or performance evaluation methodology. In addition, a major emphasis is also placed on the consideration of all the uncertainties in the design and evaluation (or lifecycle engineering, for more advanced design approaches). The various modes of characterizing the seismic damage potential lead to various PBSD approaches. The SEAOC Vision 2000 document [1], which was one of the first major publications providing a roadmap for prospective PBSD approaches, listed three broad categories for advanced seismic design approaches:

(i) Displacement-based design.
(ii) Energy-based design.
(iii) Comprehensive design considering lifecycle cost.

It should be noted that these three approaches can also be adopted for a performance-based seismic performance evaluation procedure. So far, the most commonly proposed (and even adopted in some cases) approach for PBSD is the displacement-based design approach in which a structure is designed for a target inelastic displacement, maximum (inelastic) interstorey drift, ductility demand, etc. [2]. For performance assessment of structures, the same parameters are used to define various performance levels or limit states. Among many research publications on displacement-based design methods, a small set [3–7] can be selected to represent a variety of approaches. Although an inelastic displacement-based approach to structural damage is more realistic than elastic and force-based methods, many researchers argued that the energy dissipated due to cyclic–plastic deformations in a structure during earthquakes (that is, hysteretic energy) is a better indicator of seismic structural damage [8–10], because the dissipated energy is a cumulative parameter as opposed to an instantaneous parameter, such as peak roof displacement. Ghosh and Collins [10], in their work on developing a reliability-based method considering hysteretic energy demand, suggested that more complex damage parameters, such as the Park–Ang damage index [11], which combine the cumulative energy demand with the ductility demand, would eventually prove to be even better measures of seismic damage potential. The effectiveness of using the Park–Ang and other similar damage indices has been supported by many researchers from the mid-1980s, although not always in the context of PBSD.

* Corresponding author. Tel.: +91 22 25767309; fax: +91 22 25767302.
E-mail address: sghosh@civil.iitb.ac.in (S. Ghosh).
1 Associate Professor.
2 Former doctoral student.
3 Former graduate student.

0141-0296/$ – see front matter © 2011 Elsevier Ltd. All rights reserved.
doi:10.1016/j.engstruct.2011.04.023

The first significant step in such a design method is the estimation of the demand due to the design ground hazard. With the computing facilities available today, this estimation of the Park–Ang damage index demand is not difficult, although it is computation-intensive, because the estimation involves a nonlinear response-history analysis (NLRHA) of the multi-degree-of-freedom (MDOF) model of the structure under consideration. In the conventional force-based design procedure, the computation on the designer's part is greatly reduced by the use of response spectra and an equivalent single-degree-of-freedom (ESDOF) idealization of the structure. Although this idealization gives only an approximate estimate of the actual demand, most probably it is also the reason for the huge popularity of the conventional design procedure. Such an idealization will also be useful in Park–Ang damage index-based performance evaluation and design checking methodology. Researchers have developed methods for constructing response spectra – both in the deterministic and in the probabilistic domains – for various inelastic parameters. For example, Datta and Ghosh [12] constructed uniform hazard spectra for the Park–Ang damage index (D_{PA}). The present work proposes various equivalent systems schemes for D_{PA}, which can be used in conjunction with such response spectra in a performance-based design or performance evaluation procedure based on the Park–Ang damage index.

The proposed equivalent single-degree idealization schemes are based on nonlinear static pushover analyses (NSPA) of different types. Details of these schemes are presented in Section 3, after a brief review of literature related to damage indices and equivalent systems methodology (Section 2). The proposed schemes are tested on symmetric building frames of three-, nine- and twenty-storey configurations and equivalent system estimates for a global D_{PA} are compared with the estimates from the NLRHA using the MDOF model (Section 4). Section 5 presents similar case studies to check the effectiveness of the schemes for different values of the non-dimensional parameter β. The proposed schemes, with suitable modifications, are also checked for estimating D_{PA} based on maximum interstorey drift. Significant conclusions based on this work are presented in Section 7.

2. Review of related research work

2.1. Damage indices for structures

The philosophy of PBSD, and even the conventional seismic design methods, allow controlled damage to occur in a structure in the case of a moderately strong to a very strong earthquake, while resisting collapse. Such a philosophy needs proper quantification of damage in analysis and design processes and a 'damage index' is that necessary numerical quantification of the seismic damage in a structure. In most cases, damage indices are dimensionless parameters intended to range between 0 (for an undamaged structure) to 1 (for a fully damaged or collapsed structure), with intermediate values giving some measure of the degree of partial damage. The earliest damage indices were mostly based on displacement or rotational ductility only. For example, Banon et al. [13] used the rotational ductility (μ_θ) at the end of a structural member as its damage index:

$$\mu_\theta = \frac{\theta_m}{\theta_y} = 1 + \frac{\theta_m - \theta_y}{\theta_y} \tag{1}$$

where θ_m is the maximum rotation (including both elastic and plastic rotations) under an earthquake and θ_y is the yield rotation, considering the member's antisymmetric double-curvature bending with the point of contraflexure in its mid-span. Such ductility-based damage indices fail to take into account the effects of repeated cycling including the strength and stiffness degradations under low-cycle fatigue. The 'flexural damage ratio' [13] and the 'modified flexural damage ratio' [14] are two other damage indices that also suffer from these shortcomings. One of the earliest cumulative damage parameters was the 'normalized cumulative rotation' [13], which is defined as the ratio of the sum of all plastic rotations (except for unloading parts) in inelastic springs to the yield rotation. Several other researchers [15–17] also defined similar displacement/rotation-based cumulative damage indices, while some others [18,19] followed a low-cycle fatigue-based approach to define damage indices in terms of the number of cycles to failure.

Around the same period, some other researchers [8,20] suggested incorporating cumulative hysteretic energy demand in the damage index. Park and Ang [11] defined a damage index combining both ductility and cumulative hysteretic energy demand:

$$D_{\mathrm{PA}} = \frac{d_m}{d_u} + \frac{\beta}{V_y d_u}\int \mathrm{d}E_h \tag{2}$$

where d_u = ultimate deformation (capacity) under monotonic static loading, d_m = maximum deformation (demand) under dynamic loading, $\mathrm{d}E_h$ = incremental hysteretic energy (demand), V_y = yield strength, and β = a non-negative non-dimensional parameter. Also

$$d_u = \mu d_y \tag{3}$$

where μ is the ductility capacity and d_y is the yield displacement. The Park–Ang damage index has been used in various forms over the last two and a half decades, according to the specific requirements. One of the most important modifications of this index was suggested in the third edition of the structural analysis program IDARC [21], where, for example, a member-level index was defined as

$$D_{\mathrm{PA}} = \frac{\theta_m - \theta_r}{\theta_u - \theta_r} + \frac{\beta}{M_y \theta_u}\int \mathrm{d}E_h \tag{4}$$

where θ represents the member end rotation, θ_r = recoverable rotation during unloading, and M_y = yield moment capacity. Unlike the original definition (Eq. (2)), this definition assigns '0' to the undamaged state and '1' to the fully collapsed state. Storey-level and global D_{PA} values were also defined in this work, which were obtained as weighted averages of the component level D_{PA}, where the weighting factors were based on the E_h dissipation. These modified definitions are most commonly used in today's applications of D_{PA}.

A comparison of the effectiveness of different damage indices can be found in many research publications [9,22–25], and D_{PA} is recommended as the preferred damage index. Kunnath and Jenne [24] estimated damage potential from various indices and compared them with experimental observations. The Park–Ang damage index correlated best with laboratory results. Further details on the comparison of different structural damage indices are available in the work of Williams and Sexsmith [26]. With its effectiveness in representing the actual damage state of the structure, its wide applicability to RC, steel [27] and timber [28] structures, and its applicability to different hysteresis characteristics, the Park–Ang damage index is the most preferred choice for structural damage index.

2.2. Equivalent system methodology

An equivalent single-degree-of-freedom (ESDOF) system is a simplistic representation of the actual MDOF model of a structure, based on properties of the real structure, such that the ESDOF system is capable of representing certain response(s) of the MDOF structure. Equivalent systems are used primarily in order to avoid the computation-intensive NLRHA of MDOF systems and to be able to use response spectra in day-to-day design and evaluation tasks.

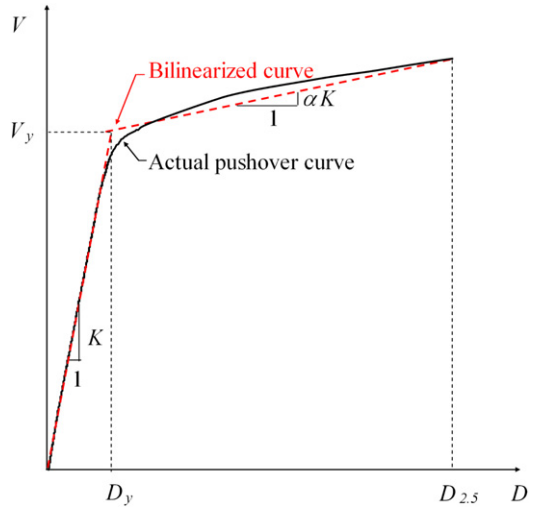

Fig. 1. Bilinear approximation of the pushover curve.

This concept of an 'equivalent' or 'generalized' system is nothing new and various alternative equivalent system methods have been proposed over the years [29,30,3,31,4,32]. The primary objective of most of these works was to estimate the displacement or ductility demand in a structure, and this was achieved by assuming a time-invariant deformation shape ($\boldsymbol{\phi}$) of the structure. In most cases, this shape was based on the fundamental (elastic) mode shape of the structure, or on the deformation shape based on a nonlinear static pushover analysis. The concept of modal pushover analysis (MPA) [33] extended this to use more than one (the fundamental) mode shape in constructing the equivalent system and it improved the displacement and force estimates, particularly for mid-rise to high-rise structures. Later, MPA-based techniques [34,35] were also successfully applied to obtain equivalent systems for plan-asymmetric building structures. Examples also exist [36] for equivalent systems for plan-asymmetric structures that are not based on MPA, but on simple pushover analysis. Makarios [37] proposed a method for optimizing the nonlinear ESDOF system for obtaining displacement demands in RC framed structures.

As many researchers argued in favour of energy-based design methods, equivalent systems were also proposed for estimating hysteretic or other energy demands in structures [38,39,10]. Prasanth et al. [40] used MPA-based equivalent systems to estimate hysteretic energy demands in framed structures and Rathore et al. [41] used both MPA- and 2D-MPA-based equivalent systems for estimating E_h demands in plan-asymmetric buildings. Although, satisfactory methods are available now for constructing equivalent systems in order to estimate both displacement/ductility and cumulative energy demands in symmetric and asymmetric frame systems, there has not been any detailed work trying to obtain equivalent systems for estimating damage indices combining the two types of seismic demand. The only significant work using equivalent systems to estimate a Park–Ang (or similar) damage index was that by Fajfar and Gašperešič [38]. In their proposed 'N2' method for RC structures, they used an NSPA-based ESDOF system to obtain the Park–Ang damage index, both at the member level and at the global level. The member-level definition of the damage index was similar to Eq. (2), with the displacements and forces replaced by rotations and moments, respectively:

$$D_{\mathrm{PA}} = \frac{\theta_m}{\theta_u} + \frac{\beta}{M_y\theta_u}\int \mathrm{d}E_h. \tag{5}$$

The global D_{PA} was obtained from a weighted average similar to the IDARC formulation [21]. They used this equivalent system to obtain D_{PA} estimates for both RC frames and shear walls. However, the focus of their work was not on measuring the effectiveness of the ESDOF system, and no detailed results were presented comparing the MDOF response to the ESDOF-based estimates. The authors, nonetheless, commented on the inefficiency of the ESDOF systems, particularly as regards not being able to incorporate the higher mode effects. Also, they did not elaborate on the basis of selecting deformation shapes ($\boldsymbol{\phi}$) for different structure types. Incorporating concepts developed over the last decade, the authors of the present work provide a detailed comparison among three alternative equivalent systems, judged by their closeness to the MDOF system response, for a variety of scenarios (where considerable higher mode effects are expected).

3. Proposed equivalent system schemes

The equivalent system schemes (ESS) proposed in this work are based on NSPA of the MDOF model of the structure, following the methodologies proposed and used by Qi and Moehle [3] and Collins et al. [4] among others. Three different ESDOF schemes are used in this work. The basic formulation of a generalized or equivalent system starts from the dynamic response of a planar MDOF cantilever-type structure subjected to horizontal base motion $\ddot{u}_g$:

$$\mathbf{m}\ddot{\mathbf{u}} + \mathbf{c}\dot{\mathbf{u}} + \mathbf{r} = -\mathbf{m}\boldsymbol{\iota}\ddot{u}_g \tag{6}$$

where $\mathbf{m}$ is the mass matrix, $\mathbf{c}$ is the damping matrix, $\mathbf{u}$ is the lateral displacement vector, $\boldsymbol{\iota}$ is the influence vector, and $\mathbf{r}$ is the restoring force vector. The generalized system replaces the displacement vector $\mathbf{u}$ with a single displacement, for example the roof displacement D, by assuming a time-invariant displacement profile or shape vector $\boldsymbol{\phi}$:

$$\mathbf{u}(t) = \boldsymbol{\phi}D(t). \tag{7}$$

In addition, the multi-degree dynamic equation is premultiplied by the same shape vector to obtain the following equation:

$$\boldsymbol{\phi}^T\mathbf{m}\boldsymbol{\phi}\ddot{D} + \boldsymbol{\phi}^T\mathbf{c}\boldsymbol{\phi}\dot{D} + \boldsymbol{\phi}^T\mathbf{r} = -\boldsymbol{\phi}^T\mathbf{m}\boldsymbol{\iota}\ddot{u}_g. \tag{8}$$

If the same shape vector is also assumed for the nonlinear static pushover analysis of the structure, then the restoring force vector can be represented by the base shear (V). On the basis of a bilinear idealization of the V versus D pushover curve (Fig. 1), one can express the base shear as a function of the roof displacement:

$$V = KG(D) \tag{9}$$

where K is the initial slope of the pushover curve and $G(.)$ is the scalar mathematical function of D describing the shape of the pushover curve (which can also include trilinear and curvilinear shapes). This reduces Eq. (8) to the equation of equilibrium for a single-degree-of-freedom system:

$$M^*\ddot{D} + C^*\dot{D} + K^*G(D) = -L^*\ddot{u}_g \tag{10}$$

where $M^* = \boldsymbol{\phi}^T\mathbf{m}\boldsymbol{\phi}$, $C^* = \boldsymbol{\phi}^T\mathbf{c}\boldsymbol{\phi}$, $K^* = \boldsymbol{\phi}^T K\mathbf{f}$, and $L^* = \boldsymbol{\phi}^T\mathbf{m}\boldsymbol{\iota}$. $\mathbf{f}$ is the force vector used in the nonlinear static pushover analysis (see Eq. (13), later). The force–deformation relation for this equivalent system can be further generalized to a hysteretic one:

$$M^*\ddot{D} + C^*\dot{D} + K^*G(D, \operatorname{sign}\dot{D}) = -L^*\ddot{u}_g. \tag{11}$$

This is the equation of motion of an inelastic single-degree system with mass M^*, damping C^* and linear elastic stiffness K^*. Dividing both sides of this equation by the mass of the ESDOF system, the dynamic equilibrium can be written in an alternative format:

$$\ddot{D} + 2\zeta\omega^*\dot{D} + (\omega^*)^2G(D, \operatorname{sign}\dot{D}) = -\Gamma^*\ddot{u}_g \tag{12}$$

where $\Gamma^* = L^*/M^*$, $(\omega^*)^2 = K^*/M^*$, and $2\zeta\omega^* = C^*/M^*$. This is the equation of motion of an inelastic SDOF oscillator with

linear elastic frequency ω^* and damping ratio ζ. After obtaining the equivalent system parameters the D_{PA} demand for the actual structure (D_{PA-ES}) is obtained from an NLRHA of the equivalent system(s) as per Eq. (11) or (12), using the proper ground motion scale factor.

The properties of the ESDOF system depends on the assumed shape vector $\boldsymbol{\phi}$ and how the pushover curve is approximated. The three different equivalent system schemes (ESS) adopted in this work, based on the general methodology presented in this section, are:

1. *ESS1*: This scheme is based on the assumption that the fundamental mode dominates the structural response to the extent that other modes' contributions can be neglected. Thus, the ESDOF system is obtained assuming $\boldsymbol{\phi} = \boldsymbol{\phi}_1$ in Eq. (7), where $\boldsymbol{\phi}_1$ is the fundamental mode shape of the structure (normalized to a roof displacement = 1). Like the concepts of modal pushover analysis, this scheme involves the implicit assumption that the structure retains the elastic (fundamental) mode shape even when it displays an inelastic response. The lateral force distribution for the NSPA is obtained as

$$\mathbf{f} = \mathbf{m}\boldsymbol{\phi}. \tag{13}$$

   The NSPA is conducted up to a 2.5% maximum interstorey drift as suggested in various previous works [10,40,41]. The pushover plot is approximated by a bilinear V versus D relation with strain-hardening. The bilinear approximation is obtained by equating the area under the pushover curve, the origin, the elastic slope and the maximum displacement point ($D_{2.5}$), as shown in Fig. 1. $D_{2.5}$ is the roof displacement corresponding to 2.5% maximum interstorey drift. Parameters K, α (strain-hardening stiffness ratio), V_y, and D_y are obtained from the bilinear plot.
2. *ESS2*: This equivalent system scheme uses the concept of modal pushover analysis and uses multiple modal ESDOF systems similarly to the method proposed by Prasanth et al. [40]. Elastic mode shapes are obtained from an eigenvalue analysis of the original structure and then NSPA is conducted for each mode, similarly to what is recommended for a single mode in ESS1. An equivalent single-degree system is obtained for each mode shape. Since D_{PA} includes both peak response (in the displacement/ductility part) and cumulative response (in the hysteretic energy part), NLRHA-based responses of multiple modal ESDOF systems are combined differently for these two parts. For the peak response part, say for a roof displacement D, an SRSS combination of modal ESDOF peak responses is used, since the modes for the test structures are found to be well-separated [33]. A CQC-based combination can also be used with a wider scope of application. The E_h demand on the structure is obtained by a simple summation of individual hysteretic energy demands of modal equivalent systems [40]. In these combinations, only the first two modal ESDOF systems are used for the three-storey test frame and the first five ESDOF systems are used for the nine- and twenty-storey test frames (discussed later). On the basis of recommendations from previous research works [33,40,41], even five modes may be a conservative assumption. In retrospect, one can interpret ESS1 as a first-mode-only variant of ESS2.
3. *ESS3*: Similarly to ESS1, ESS3 is also based on a single equivalent system. However, the shape vector is not a modal one. The NSPA is conducted using the lateral force distribution ($\mathbf{f}$) recommended by IBC 2006 [42]. Thus, obtaining ESS3 does not need any eigenvalue analysis. The shape vector ($\boldsymbol{\phi}$) is obtained from the deformation shape during the linear elastic response in NSPA. In terms of bilinearization, obtaining the ESDOF system parameters, and estimating the structure's D_{PA} demand, the same steps are followed as in ESS1.

Table 1
ESDOF parameters for the three ESS for the case study frames.

	Mode	ω^* (rad/s)	M^* (kNs^2/m)	Γ^*
3-storey	1	5.68	912	1.27
	2	17.5	2200	0.330
	IBC	5.68	912	1.27
9-storey	1	2.78	2000	1.37
	2	7.34	1730	0.531
	3	15.2	2890	0.241
	4	18.2	4150	0.116
	5	27.6	7480	0.057
	IBC	3.11	1250	1.49
20-storey	1	1.65	2330	1.38
	2	4.76	1960	0.576
	3	8.23	1780	0.330
	4	11.4	2010	0.222
	5	15.3	2430	0.152
	IBC	1.90	1320	1.56

Table 1 shows sample values of ESDOF parameters for the three different ESS for the three test structures. Note that only Mode 1 data are used by ESS1 while ESS2 uses data for Modes 1–5. The ESDOF parameters corresponding to 'IBC' is for ESS3. The test structures considered in the three case studies in the next three sections are the "pre-Northridge" design of the three-, nine-, and twenty-storey "SAC Steel" moment frame buildings from Los Angeles, USA. These frames have been used in various similar research works in the recent past [33,34,43,10,40], and the details, that are available in a report [44], are avoided here for brevity. Since these are symmetric-in-plan buildings, only the North–South frame of each building is considered for analysis.

4. Case studies I: for a global D_{PA}

For the first set of case studies checking the effectiveness of the proposed ESS, the modified Park–Ang damage index for the MDOF model of the study frame is defined as

$$D_{PA} = \frac{D_m - D_y}{D_u - D_y} + \frac{\beta}{V_y D_u}\int \mathrm{d}E_h \tag{14}$$

where D_m = maximum roof displacement based on NLRHA of the MDOF model, D_y = yield roof displacement based on the bilinearized pushover plot, and D_u = roof displacement capacity = μD_y with μ being the pre-determined displacement ductility capacity. It should be noted that ideally Eq. (14) should be applied to a cantilever with D_m and D_y representing its displacements at the free end. This concept is extended here to a planar multi-storey frame as the behaviour of the planar frame subjected to horizontal earthquake excitation is similar to that of a vertical cantilever fixed at the base. An alternative definition for D_y can be based on the first yield from a NLRHA. This first yield (formation of the first plastic hinge for these structures) will vary depending on the ground motion selected for the NLRHA. Since the denominators in Eq. (14) should represent capacity parameters for the structure, a D_y based on the NSPA of the structure is preferred to ensure that these capacity parameters remain properties of the structure only, and not of the ground motion considered. Three different ductility capacities are considered in all the case studies: 4, 6, and 7.5. In E_h, the total hysteretic energy demand in all the plastic hinge locations is included. On the basis of the recommendation of Park et al. [27], the factor β for steel structures is considered as 0.025. In Section 5, the sensitivity of these ESS to β is studied in detail. The definition as per Eq. (14) is termed the 'global' D_{PA}, because it considers only the roof displacement and the total energy demand for the structure. Further studies on a more localized damage index are presented in Section 6.

Table 2
Details of the strong motion records used.

No.	Earthquake	Date	Station	Orientation
1	Chi-Chi	Sep 21, 1999	Yunlin–Tsaoling	090
2	Northridge	Jan 17, 1994	Sylmar Olive View Med. FF	360
3	Chi-Chi	Sep 21, 1999	Taichung Wufeng School	090
4	Cape Mendocino	Apr 25, 1992	Cape Mendocino	000
5	Loma Prieta	Oct 18, 1989	UCSC Station 16	000
6	San Fernando	Feb 09, 1971	Pacoima Dam	165
7	Tabas	Sep 16, 1978	9101 Tabas	LN
8	Northridge	Jan 17, 1994	Tarzana Cedar Hill Nursery A	090
9[a]	Northridge	Jan 17, 1994	Sylmar Converter	142
10	Northridge	Jan 17, 1994	Newhall Fire Station	360
11	Northridge	Jan 17, 1994	Newhall Fire Station	090
12	Parkfield	Jun 28, 1966	Parkfield	
13	Kobe	Jan 16, 1995	KJMA	000
14	Northridge	Jan 17, 1994	Sylmar Olive View Med. FF	090
15	Kobe	Jan 16, 1995	KJMA	090
16	Loma Prieta	Oct 18, 1989	UCSC Station 16	090
17	Northridge	Jan 17, 1994	Arleta Nordhoff Fire Station	090
18[a]	Northridge	Jan 17, 1994	Newhall Fire Station	090
19	Tabas	Sep 16, 1978	9101 Tabas	TR
20	Gazli	May 17, 1976	Karakyr	090

[a] 9 gives the velocity-corrected data for the same record as 18.

Table 3
Comparison of MDOF- and ESDOF-based D_{PA} estimates for all ESS for the three-storey building, with $\beta = 0.025$.

Record No.	$\mu = 4.0$				$\mu = 6.0$				$\mu = 7.5$			
	MDOF	ESS1	ESS2	ESS3	MDOF	ESS1	ESS2	ESS3	MDOF	ESS1	ESS2	ESS3
1	1.00	1.00	1.00	1.00	1.00	1.00	1.00	1.00	1.00	1.00	1.00	1.00
2	0.993	1.00	1.00	1.00	0.599	0.703	0.709	1.00	0.461	0.542	0.547	1.00
3	1.00	1.00	1.00	1.00	0.605	0.832	0.833	1.00	0.466	0.641	0.641	1.00
4	0.844	1.00	1.00	1.00	0.508	0.758	0.763	1.00	0.391	0.583	0.587	1.00
5	0.763	1.00	1.00	1.00	0.463	0.883	0.884	1.00	0.358	0.681	0.682	1.00
6	1.00	1.00	1.00	1.00	0.742	0.899	0.902	1.00	0.572	0.693	0.695	1.00
7	1.00	1.00	1.00	1.00	0.639	1.00	1.00	1.00	0.493	0.833	0.834	1.00
8	1.00	1.00	1.00	1.00	0.627	0.769	0.798	0.831	0.483	0.592	0.616	0.639
9	1.00	1.00	1.00	1.00	1.00	1.00	1.00	1.00	1.00	0.832	0.832	0.969
10	1.00	1.00	1.00	1.00	0.844	0.872	0.874	1.00	0.650	0.672	0.674	1.00
11	0.288	0.573	0.582	1.00	0.174	0.346	0.352	0.634	0.134	0.267	0.271	0.487
12	1.00	1.00	1.00	1.00	0.706	1.00	1.00	1.00	0.543	0.994	0.994	1.00
13	0.708	0.901	0.911	0.969	0.429	0.546	0.552	0.582	0.331	0.422	0.426	0.448
14	0.798	1.00	1.00	1.00	0.480	0.653	0.654	1.00	0.370	0.503	0.503	1.00
15	0.736	1.00	1.00	1.00	0.444	0.678	0.681	0.665	0.343	0.523	0.525	0.512
16	0.444	0.612	0.612	0.988	0.268	0.368	0.368	0.593	0.206	0.283	0.284	0.456
17	0.380	0.392	0.393	1.00	0.229	0.236	0.237	0.664	0.176	0.182	0.182	0.511

All the NLRHA and NSPA conducted for the three case studies presented in this paper are performed using the analysis platform DRAIN-2DX [45]. The moment frames are modelled using elastic–perfectly plastic steel with a yield stress of 345 MPa (50 ksi). Beam and column members are modelled with a Type 02 nonlinear beam–column element with proper P–M interactions at each possible plastic hinge locations. A Rayleigh damping of 5% is assigned to the first two modes of vibration. The rigid floor diaphragm effect is assumed for all the floors where masses are lumped. The stiffness contribution from the gravity frames, flexibility of the joint panel zones, strength and/or stiffness degradation in successive displacement cycles, and secondary moment effects are neglected.

In order to measure the effectiveness of an ESS, the ESDOF demand (D_{PA-ES}) is compared with the MDOF demand (D_{PA-M}), under various ground motion scenarios. The effectiveness of an ESS is measured by a bias factor

$$N = \frac{D_{PA-M}}{D_{PA-ES}} \tag{15}$$

for every structure, for every ground motion scenario and for the selected μ values. A total of 20 strong ground motion records are considered for this study. It should be noted that 20 records may not be sufficient to avoid the sensitivity of the result statistics to record selection. A larger set of ground motions, with specific emphasis on the nature of earthquake and ground characteristics, would produce better statistics that can be directly used in design standards. However, considering that the primary objective of the case studies presented here is to check the effectiveness of the ESS for a variety of records, frame heights, ductility range, and β values, and over a large range of D_{PA} demands, the sample results presented in this paper are deemed adequate. Table 2 provides details of these records. These records are identified later using only the serial number that appears corresponding to each record in this table. For the nine- and twenty-storey frames, many times the original records do not cause any damage ($D_{PA-M} = 0$), or cause a negligible amount of damage ($D_{PA} < 0.100$) which is not of interest from the perspective of a damage-based/inelastic design/performance evaluation approach. Therefore, the original ground motions are suitably scaled up in order to produce significant damage in the structure so that these can be included in the ESS statistics. Nevertheless, only (scaled) records 1–17 are used for the three-storey frame, (scaled) records 1–13, 18, and 19 are used for the nine-storey frame, and (scaled) records 1–8 and 18-20 are used for the twenty-storey frame. To maintain some uniformity, all the original acceleration data are scaled by a factor of 1.5 for the different case studies presented here. Table 3 presents a sample comparison between the Park–Ang damage index estimated using

Table 4
Bias factor (N) values for all ESS for the three-storey building, with $\beta = 0.025$.

Record No.	$\mu = 4.0$			$\mu = 6.0$			$\mu = 7.5$		
	ESS1	ESS2	ESS3	ESS1	ESS2	ESS3	ESS1	ESS2	ESS3
1	1.00	1.00	1.00	1.00	1.00	1.00	1.00	1.00	1.00
2	0.993	0.993	0.993	0.852	0.844	0.599	0.852	0.844	0.461
3	1.00	1.00	1.00	0.727	0.727	0.605	0.727	0.727	0.466
4	0.844	0.844	0.844	0.670	0.665	0.508	0.670	0.665	0.391
5	0.763	0.763	0.763	0.524	0.524	0.463	0.525	0.524	0.358
6	1.00	1.00	1.00	0.825	0.823	0.742	0.826	0.824	0.572
7	1.00	1.00	1.00	0.639	0.639	0.639	0.592	0.591	0.493
8	1.00	1.00	1.00	0.815	0.785	0.754	0.816	0.785	0.756
9	1.00	1.00	1.00	1.00	1.00	1.00	1.20	1.20	1.03
10	1.00	1.00	1.00	0.968	0.966	0.844	0.968	0.965	0.650
11	0.502	0.494	0.288	0.503	0.495	0.275	0.503	0.495	0.275
12	1.00	1.00	1.00	0.706	0.706	0.706	0.547	0.547	0.543
13	0.785	0.777	0.731	0.785	0.776	0.737	0.785	0.776	0.739
14	0.798	0.798	0.798	0.735	0.735	0.480	0.735	0.735	0.370
15	0.736	0.736	0.736	0.655	0.652	0.668	0.655	0.653	0.669
16	0.726	0.725	0.449	0.727	0.726	0.451	0.727	0.726	0.452
17	0.970	0.967	0.380	0.969	0.967	0.345	0.969	0.966	0.345

Table 5
Bias factor (N) values for all ESS for the nine-storey building, with $\beta = 0.025$.

Record No.	$\mu = 4.0$			$\mu = 6.0$			$\mu = 7.5$		
	ESS1	ESS2	ESS3	ESS1	ESS2	ESS3	ESS1	ESS2	ESS3
1	1.00	1.00	1.00	1.00	1.00	1.00	1.00	1.00	1.00
2	0.806	0.800	0.646	0.808	0.802	0.648	0.809	0.802	0.649
3	0.784	0.782	0.592	0.790	0.783	0.356	0.794	0.798	0.274
4	1.57	1.45	1.53	1.57	1.45	1.53	1.57	1.45	1.53
5	1.00	1.00	1.00	0.621	0.621	0.621	0.495	0.498	0.483
6	0.920	0.897	0.920	0.921	0.898	0.922	0.922	0.898	0.923
7	1.20	1.16	1.30	1.20	1.16	1.30	1.21	1.16	1.30
8	0.799	0.756	0.640	0.802	0.757	0.643	0.803	0.754	0.644
9	0.809	0.747	0.696	0.814	0.750	0.702	0.816	0.751	0.704
10	0.949	0.912	0.974	0.952	0.914	0.977	0.953	0.915	0.978
11	0.990	0.925	0.961	0.992	0.927	0.964	0.992	0.926	0.965
12	1.00	1.00	1.00	0.731	0.731	0.731	0.701	0.707	0.563
13	0.811	0.485	0.563	0.814	0.489	0.569	0.815	0.490	0.571
18	0.985	0.920	0.953	0.986	0.921	0.955	0.987	0.922	0.956
19	0.653	0.653	0.653	0.571	0.572	0.553	0.571	0.573	0.554

Table 6
Bias factor (N) values for all ESS for the twenty-storey building, with $\beta = 0.025$.

Record No.	$\mu = 4.0$			$\mu = 6.0$			$\mu = 7.5$		
	ESS1	ESS2	ESS3	ESS1	ESS2	ESS3	ESS1	ESS2	ESS3
1	1.00	1.00	1.00	1.00	1.00	1.00	1.00	1.00	1.00
2	0.910	0.812	1.03	0.911	0.813	1.03	0.911	0.813	1.04
3	0.812	0.812	0.812	0.668	0.667	0.489	0.668	0.667	0.376
4	0.734	0.693	0.385	0.735	0.695	0.387	0.736	0.695	0.387
5	1.12	1.02	1.04	1.12	1.02	1.05	1.12	1.02	1.05
6	0.846	0.762	0.744	0.849	0.763	0.746	0.850	0.764	0.747
7	1.04	0.958	0.849	1.04	0.959	0.849	1.04	0.959	0.849
8	1.02	0.644	0.588	1.03	0.648	0.595	1.03	0.650	0.598
18	2.00	1.79	1.78	2.00	1.79	1.78	2.00	1.79	1.78
19	0.218	0.218	0.218	0.142	0.141	0.136	0.144	0.143	0.122
20	0.568	0.563	0.440	0.567	0.562	0.440	0.567	0.561	0.439

the MDOF and the three different ESS for the three-storey frame for all the earthquakes and for the three selected μ values. This table illustrates that the ESS are tested for a large range of D_{PA-M} values from 0.134 to 1.00. From these D_{PA} values, the bias factor is calculated for each record and ductility capacity. Tables 4–6 present the bias factor values in detail for each earthquake for the three test structures. The summary statistics (Table 7), in terms of the mean, standard deviation (SD), coefficient of variation (CoV), and maximum and minimum values, present an overall picture of the level of accuracy for a selected ESS. A bias value of 1.0 signifies that the ESS is as accurate as the NLRHA, from a D_{PA} perspective. $N > 1.0$ signifies an underestimation by the ESS and vice versa. Overall, a mean bias close to 1.0 and low SD and CoV values indicate that the ESS is very effective. The summary statistics are presented separately for the three ductility capacities. However. it can be noted from these tables that the overall statistics are not very different for different μ values, and one can also consider these three sets for each ESS together.

Figs. 2–4 illustrate this bias (N) for each earthquake, where every plot is for a selected ductility capacity of the structure. The earthquake serial numbers are the same as those presented in Table 2. These bar charts give a clear idea of the comparative measure of effectiveness, among the three ESS proposed. The vertical line at $N = 1$ presents the ideal response from an ESS. A point towards right of that line indicates an underestimation by the ESS for the record under consideration, and vice versa. These plots,

Table 7
Bias (N) statistics summary for all ESS for the three-, nine- and twenty-storey buildings, with $\beta = 0.025$.

		$\mu = 4.0$			$\mu = 6.0$			$\mu = 7.5$		
		ESS1	ESS2	ESS3	ESS1	ESS2	ESS3	ESS1	ESS2	ESS3
3-storey	Mean	0.889	0.888	0.822	0.771	0.766	0.636	0.771	0.766	0.563
	SD	0.148	0.150	0.240	0.154	0.154	0.205	0.189	0.189	0.220
	CoV	0.167	0.169	0.292	0.200	0.201	0.322	0.245	0.247	0.391
	Max.	1.00	1.00	1.00	1.00	1.00	1.00	1.20	1.20	1.03
	Min.	0.502	0.494	0.288	0.503	0.495	0.275	0.503	0.495	0.275
9-storey	Mean	0.952	0.899	0.895	0.905	0.851	0.832	0.896	0.842	0.807
	SD	0.217	0.223	0.273	0.244	0.237	0.306	0.257	0.248	0.330
	CoV	0.228	0.249	0.305	0.269	0.279	0.369	0.287	0.295	0.410
	Max.	1.57	1.45	1.53	1.57	1.45	1.53	1.57	1.45	1.53
	Min.	0.653	0.485	0.564	0.571	0.489	0.356	0.495	0.490	0.274
20-storey	Mean	0.933	0.842	0.809	0.915	0.823	0.773	0.916	0.824	0.763
	SD	0.436	0.387	0.425	0.456	0.404	0.447	0.456	0.404	0.458
	CoV	0.467	0.460	0.526	0.498	0.491	0.579	0.498	0.490	0.600
	Max.	2.00	1.79	1.78	2.00	1.79	1.78	2.00	1.79	1.78
	Min.	0.218	0.218	0.218	0.142	0.141	0.136	0.144	0.143	0.122

along with Tables 4–6, show that the proposed equivalent system schemes are effective in estimating the MDOF D_{PA} demand on the basis of Eq. (14). Not all schemes are equally effective for each building, each μ, and each earthquake scenario; however, in an overall sense, these schemes are deemed to be usable in practical applications.

The bias factor summary (Table 7) and these figures are useful in comparing the effectiveness of different ESS in estimating the actual D_{PA}. For the three-storey building, all the three ESS give very similar results in terms of the mean bias for a given μ (except for one or two very low mean biases for ESS3, indicating a major overestimation by that ESS). However, when their SD and CoV are taken into consideration, ESS1 and ESS2 are found to be more reliable. One should also note that for low μ values, the estimates are better for all the three ESS. This is primarily because for a majority of selected records, the three-storey building reaches its capacity ($D_{PA} = 1.0$) for both the original MDOF model and the approximate ESS models, resulting in $N = 1$ ($D_{PA} \not> 1.0$). For $\mu = 7.5$ the mean bias moves further away from the ideal value of 1.0 and the CoV are higher. ESS1 is found to provide the best results among the three. However, the difference between ESS1 and ESS2 is insignificant since the three-storey frame's behaviour is hardly affected by the second elastic mode, which is incorporated in ESS2 in addition to the fundamental mode considered for ESS1. For the nine-storey frame, the mean values are mostly better than what they are for the three-storey frame. Specifically for ESS1, the mean bias is very close to its ideal value 1.0, with ESS2 and ESS3 behind it, in that order. However, the CoV values show that all the ESS are less consistent for the nine-storey frame compared to the three-storey frame. ESS1 is found, again, to provide the best overall results. Unlike the three-storey frame, results for ESS1 and ESS2 are different, primarily in terms of the mean bias. This is because ESS2 includes higher mode effects, which are not negligible for the nine-storey frame.

A closer look at how D_{PA} is obtained in these two schemes explains why ESS1 gives better results even for the nine-storey frame. The primary two components for D_{PA} are the roof displacement (D_m) and the hysteretic energy (E_h) demands. Earlier studies [10,40] show that a first mode-based scheme, similar to ESS1, underestimates the actual (that is, based on MDOF) E_h, and this underestimation is greater for taller structures where higher mode effects are also significant. This underestimation, specifically for the high-rises, reduces for a multi-mode-based scheme, similar to ESS2, because it adds the higher mode contributions to the E_h demand of the first mode-based scheme. Roof displacement demands, on the other hand, tend to overestimate the actual demand and this shortcoming becomes even worse when higher mode contributions are combined (through SRSS or CQC) with the D_m demand from the first mode-based scheme. Obviously, the differences between ESS1 and ESS2 are more prominent for the taller frames. For example, ESS1 has a very acceptable mean bias of 0.952 for the nine-storey frame with $\mu = 4$, due to a balancing of the underestimation of E_h and the overestimation of D_m. Contributions from higher modes increase both E_h and D_m in ESS2, and in turn D_{PA-ES}. Therefore, finally the mean N goes down for ESS2 (to 0.899 in this case), making ESS1 the best scheme, although it may intuitively seem that the opposite is more likely for taller frames. As μ increases, the results deteriorate for all the ESS, for this nine-storey frame as well.

For the twenty-storey frame, similar trends continue, with ESS1 providing the best estimates overall, and ESS2 and ESS3 following it, in that order. As one can expect (on the basis of the explanation provided in the previous paragraph), the difference between the results of ESS1 and ESS2 is even greater for the twenty-storey frame. There is a significant increase in the CoV values overall, signifying that estimates for the twenty-storey frame are less consistent. This is also evident from the wide scatter in the bar diagrams in Fig. 4. The maximum and minimum N values cover a much wider range compared to the bias for the other two study frames.

5. Case studies II: for a global D_{PA} with different values of β

The value of the non-negative non-dimensional constant β (Eq. (14)) may have a significant influence on the damage index D_{PA} [38]. β is used in the definition of D_{PA} to account for the material–structural behaviour under cyclic load reversals (low-cycle fatigue). The value of this parameter is calibrated from experimental results for the typical structural system under consideration with predefined collapse (and other limit states). The calibration of β was discussed in detail by various authors, such as Park et al. [46] and van de Lindt [28]. Also, empirical formulas were proposed for calculating β [11]. A low value of β reduces the influence of low-cycle fatigue and the seismic damage is governed by the maximum displacement (or rotation) demand. When β is high the cumulative plastic damage becomes the cause of seismic failure. Typically, a high β value represents a poorly designed (and detailed) structure commonly available in old building stock.

Over the last two and a half decades, researchers have proposed and used various β values, ranging from 0.025 for steel structures and 0.05 for RC structures [27] to 0.23 for steel structures [47] and 0.24 for RC structures [48]. For RC structures, a value of 0.15, proposed originally by Park et al. [46], was used later in many research works. In Section 4, β is considered to be 0.025 for steel

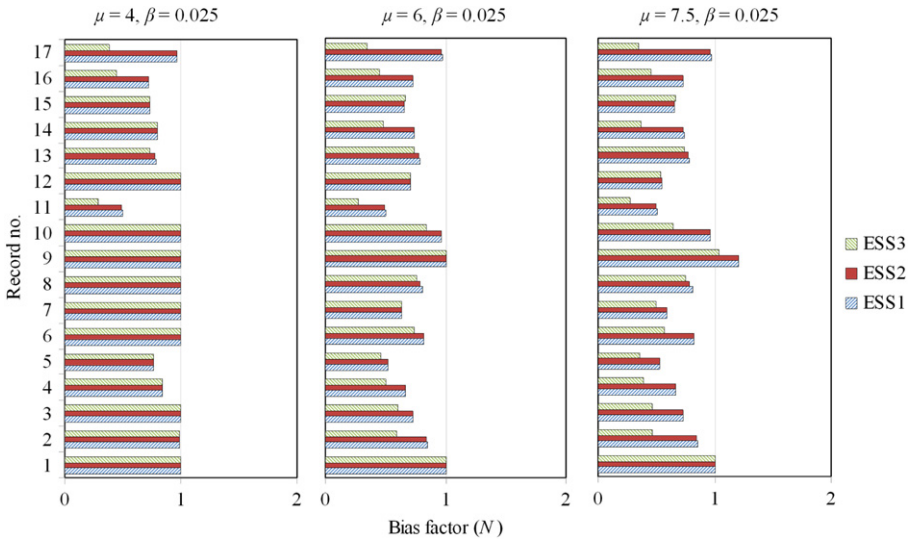

Fig. 2. Bar charts for the bias factor (N) for the three-storey frame, for $\beta = 0.025$.

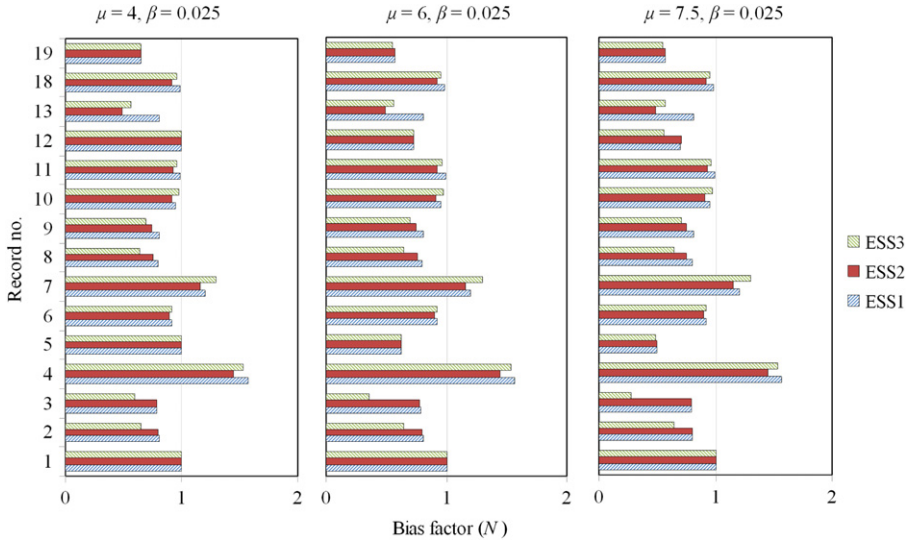

Fig. 3. Bar charts for the bias factor (N) for the nine-storey frame, for $\beta = 0.025$.

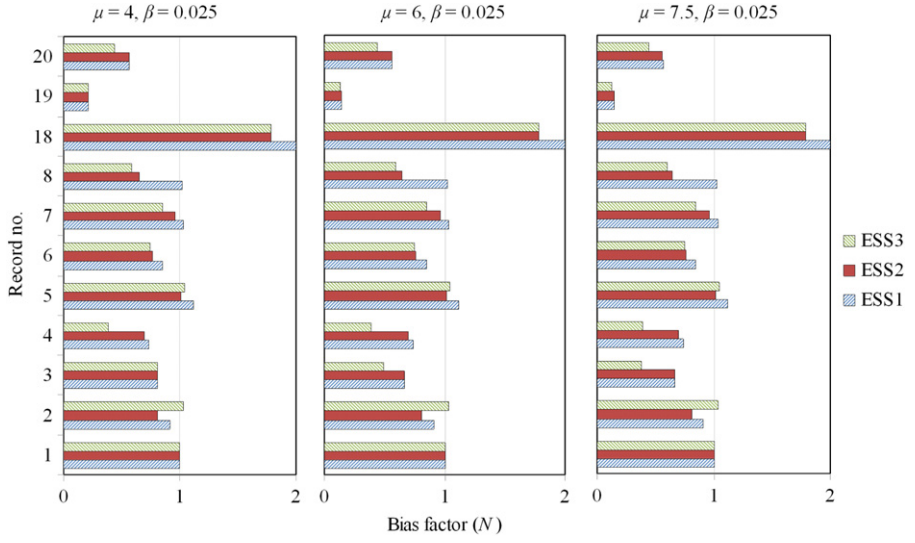

Fig. 4. Bar charts for the bias factor (N) for the twenty-storey frame, for $\beta = 0.025$.

Table 8
Bias (N) statistics summary for the three-storey building with varying β values.

β		$\mu = 4.0$			$\mu = 6.0$			$\mu = 7.5$		
		ESS1	ESS2	ESS3	ESS1	ESS2	ESS3	ESS1	ESS2	ESS3
	Mean	0.881	0.880	0.811	0.765	0.762	0.620	0.753	0.765	0.548
	SD	0.153	0.154	0.244	0.158	0.159	0.206	0.192	0.197	0.219
0.01	CoV	0.173	0.175	0.301	0.207	0.208	0.332	0.255	0.257	0.399
	Max.	1.00	1.00	1.00	1.00	1.00	1.00	1.18	1.23	1.02
	Min.	0.506	0.467	0.534	0.508	0.469	0.351	0.491	0.469	0.270
	Mean	0.889	0.888	0.822	0.771	0.766	0.636	0.771	0.766	0.563
	SD	0.148	0.150	0.240	0.154	0.154	0.205	0.189	0.189	0.220
0.025	CoV	0.167	0.169	0.292	0.200	0.201	0.322	0.245	0.247	0.391
	Max.	1.00	1.00	1.00	1.00	1.00	1.00	1.20	1.20	1.03
	Min.	0.502	0.494	0.288	0.503	0.495	0.275	0.503	0.495	0.275
	Mean	0.899	0.898	0.838	0.780	0.774	0.663	0.773	0.767	0.587
	SD	0.140	0.143	0.232	0.147	0.147	0.205	0.173	0.173	0.219
0.05	CoV	0.156	0.159	0.277	0.189	0.190	0.310	0.224	0.225	0.374
	Max.	1.00	1.00	1.00	1.00	1.00	1.00	1.12	1.12	1.02
	Min.	0.509	0.499	0.308	0.511	0.499	0.295	0.511	0.500	0.296
	Mean	0.911	0.910	0.853	0.790	0.781	0.690	0.776	0.767	0.610
	SD	0.132	0.135	0.226	0.142	0.142	0.207	0.161	0.159	0.220
0.075	CoV	0.145	0.148	0.265	0.180	0.181	0.301	0.207	0.208	0.361
	Max.	1.00	1.00	1.00	1.00	1.00	1.00	1.05	1.05	1.02
	Min.	0.516	0.502	0.329	0.518	0.503	0.314	0.519	0.504	0.317
	Mean	0.924	0.923	0.868	0.800	0.790	0.716	0.780	0.769	0.634
	SD	0.128	0.131	0.222	0.135	0.135	0.211	0.152	0.150	0.222
0.1	CoV	0.138	0.142	0.256	0.169	0.171	0.294	0.195	0.195	0.351
	Max.	1.00	1.00	1.00	1.00	1.00	1.00	1.00	1.00	1.01
	Min.	0.522	0.505	0.350	0.524	0.507	0.334	0.525	0.507	0.337
	Mean	0.955	0.953	0.914	0.863	0.859	0.848	0.826	0.804	0.773
	SD	0.118	0.124	0.191	0.134	0.141	0.236	0.136	0.127	0.261
0.25	CoV	0.124	0.130	0.209	0.155	0.164	0.278	0.165	0.158	0.337
	Max.	1.00	1.00	1.00	1.00	1.00	1.23	1.06	1.00	1.24
	Min.	0.547	0.520	0.475	0.551	0.521	0.437	0.552	0.522	0.441

structures on the basis of the recommendation of Park et al. [27]. These values of β were used for both definitions of D_{PA} as per Eqs. (2) and (14). Instead of adopting or calibrating any specific value for this parameter, the sensitivity of the proposed ESS is studied here for the widest possible range of realistic β values. Therefore, the case study described in Section 4 is now extended for the following β values: 0.01, 0.05, 0.075, 0.1 and 0.25. Tables presented in this section repeat the data for $\beta = 0.025$ from the previous section for a better comparison. These case studies (set II) are based on the same three building frames as the previous set of studies discussed in Section 4, with the same set of scaled earthquake records for each frame. The definition of D_{PA} and the analyses used to obtain its parameters remain unchanged.

Results obtained from these analysis are interpreted and compared in terms of the bias factor, N. For brevity, only the summary statistics for this factor are presented in three tables for the three structures (Tables 8–10). Each of these summary tables includes results for one study frame, all the three ESS, all the three ductility capacity values and six β values. In general, the trends observed for $\beta = 0.025$ are repeated for other β values, as well. For all the buildings, the general trend is that the estimations improve with each increasing β. This improvement in the D_{PA} estimation is evident from the mean bias increasing towards the ideal value 1.0 and a reduction in the coefficient of variation. Although this does not happen for every increase of β, for every μ, for every ESS and for every building frame, the majority of the bias statistics summary follows this trend. For example, for the three-storey frame, for $\mu = 4$, the mean bias for ESS1 increases from 0.881 for $\beta = 0.01$, monotonically at every increase in β, to 0.955 for $\beta = 0.25$. The coefficient of variation also reduces, monotonically, from 0.173 for $\beta = 0.01$ to 0.124 for $\beta = 0.25$. The reduction in the CoV is of greater importance as it indicates a better level of consistency in estimating the real demand. For the nine- and twenty-storey frames, the mean bias increases slightly beyond 1.0 in a few cases at $\beta = 0.25$, indicating a minor underestimation of the actual D_{PA}. One should, however, note that these underestimations for $\beta = 0.25$ are still the best estimates among all the β values in terms the mean bias. In addition, and more importantly, the CoV values are usually the lowest for $\beta = 0.25$. The ESS3 estimates for higher β values are very good and deemed usable, as opposed to the ESS3 estimates at lower β values, particularly for $\mu = 7.5$. ESS1 comes out as the best ESS overall, with the other two providing very good estimates at higher β values. The improvement observed at higher β values is due to the fact that with increased β, the E_h part has a larger share in D_{PA} (Eq. (14)). At low β values, D_{PA} is dominated by the maximum displacement (D_m) part, which, as Prasanth et al. [40] reported, tends to be overestimated by these ESS. These ESS, on the other hand, tends to underestimate the E_h demand. Thus, when the share of E_h is increased with increase in β, the mean bias increases, moving towards the ideal value 1.0. Prasanth et al. [40] also observed that the E_h estimates are more consistent with a lower coefficient of variation of the bias factor than the D_m estimates. This explains the reduction (even if it is not a major reduction) in the deviation in N for D_{PA} estimates at higher β values. A sample scatterplot for the nine-storey frame for $\beta = 0.25$ is provided in Fig. 5 for a comparison with the scatterplot presented earlier for $\beta = 0.025$ (Fig. 3).

6. Case studies III: D_{PA} based on the interstorey drift ratio

Although the roof displacement of a multi-storey building frame is very commonly used for characterizing the seismic demand for a given earthquake record, the response quantity most preferred as a displacement-based demand is the maximum interstorey drift ratio among all the floors. This peak interstorey

Table 9
Bias (N) statistics summary for the nine-storey building with varying β values.

β		$\mu = 4.0$			$\mu = 6.0$			$\mu = 7.5$		
		ESS1	ESS2	ESS3	ESS1	ESS2	ESS3	ESS1	ESS2	ESS3
	Mean	0.936	0.893	0.882	0.888	0.844	0.816	0.879	0.835	0.792
	SD	0.259	0.231	0.279	0.279	0.245	0.310	0.289	0.255	0.332
0.01	CoV	0.276	0.259	0.316	0.315	0.290	0.379	0.329	0.305	0.420
	Max.	1.63	1.46	1.53	1.63	1.46	1.53	1.63	1.46	1.53
	Min.	0.506	0.467	0.471	0.508	0.469	0.351	0.491	0.469	0.270
	Mean	0.952	0.899	0.895	0.905	0.851	0.832	0.896	0.842	0.807
	SD	0.217	0.223	0.273	0.244	0.237	0.306	0.257	0.248	0.330
0.025	CoV	0.228	0.249	0.305	0.269	0.279	0.369	0.287	0.295	0.410
	Max.	1.57	1.45	1.53	1.57	1.45	1.53	1.57	1.45	1.53
	Min.	0.653	0.485	0.564	0.571	0.489	0.356	0.495	0.490	0.274
	Mean	1.00	0.872	0.916	0.937	0.820	0.856	0.927	0.809	0.831
	SD	0.228	0.217	0.264	0.247	0.226	0.302	0.262	0.237	0.327
0.05	CoV	0.228	0.249	0.288	0.263	0.275	0.352	0.282	0.293	0.394
	Max.	1.61	1.39	1.54	1.61	1.38	1.54	1.61	1.38	1.54
	Min.	0.696	0.466	0.604	0.598	0.467	0.364	0.516	0.468	0.281
	Mean	0.978	0.917	0.937	0.937	0.873	0.879	0.926	0.861	0.854
	SD	0.229	0.200	0.256	0.253	0.215	0.297	0.268	0.229	0.325
0.075	CoV	0.234	0.219	0.273	0.270	0.246	0.338	0.290	0.266	0.381
	Max.	1.61	1.42	1.55	1.60	1.42	1.55	1.60	1.42	1.55
	Min.	0.617	0.540	0.617	0.618	0.548	0.373	0.531	0.527	0.287
	Mean	0.975	0.908	0.938	0.921	0.850	0.868	0.902	0.830	0.836
	SD	0.229	0.195	0.255	0.271	0.225	0.310	0.295	0.247	0.343
0.1	CoV	0.234	0.215	0.272	0.294	0.264	0.357	0.327	0.297	0.410
	Max.	1.60	1.41	1.56	1.60	1.40	1.56	1.59	1.40	1.56
	Min.	0.657	0.564	0.629	0.501	0.501	0.381	0.404	0.404	0.294
	Mean	1.07	0.966	1.06	1.04	0.934	1.02	1.02	0.914	0.991
	SD	0.180	0.151	0.224	0.207	0.161	0.283	0.231	0.177	0.319
0.25	CoV	0.169	0.157	0.212	0.199	0.172	0.278	0.226	0.193	0.322
	Max.	1.57	1.35	1.60	1.56	1.34	1.60	1.56	1.34	1.60
	Min.	0.830	0.677	0.704	0.726	0.694	0.431	0.698	0.698	0.334

Table 10
Bias (N) statistics summary for the twenty-storey building with varying β values.

β		$\mu = 4.0$			$\mu = 6.0$			$\mu = 7.5$		
		ESS1	ESS2	ESS3	ESS1	ESS2	ESS3	ESS1	ESS2	ESS3
	Mean	0.850	0.776	0.739	0.811	0.739	0.684	0.800	0.729	0.663
	SD	0.290	0.270	0.316	0.285	0.261	0.312	0.279	0.254	0.314
0.01	CoV	0.341	0.347	0.427	0.351	0.353	0.455	0.349	0.348	0.474
	Max.	1.24	1.16	1.16	1.11	1.01	1.03	1.11	1.01	1.03
	Min.	0.175	0.175	0.175	0.115	0.115	0.107	0.116	0.115	0.098
	Mean	0.933	0.842	0.809	0.915	0.823	0.773	0.916	0.824	0.763
	SD	0.436	0.387	0.425	0.456	0.404	0.447	0.456	0.404	0.458
0.025	CoV	0.467	0.460	0.526	0.498	0.491	0.579	0.498	0.490	0.600
	Max.	2.00	1.79	1.78	2.00	1.79	1.78	2.00	1.79	1.78
	Min.	0.218	0.218	0.218	0.142	0.141	0.136	0.144	0.143	0.122
	Mean	0.892	0.804	0.777	0.848	0.762	0.721	0.838	0.752	0.699
	SD	0.284	0.250	0.302	0.289	0.248	0.305	0.283	0.239	0.312
0.05	CoV	0.319	0.311	0.388	0.341	0.325	0.423	0.338	0.318	0.446
	Max.	1.30	1.20	1.20	1.14	1.02	1.08	1.14	1.02	1.08
	Min.	0.290	0.290	0.290	0.184	0.184	0.184	0.187	0.186	0.158
	Mean	0.916	0.820	0.801	0.870	0.775	0.743	0.859	0.764	0.720
	SD	0.282	0.239	0.295	0.292	0.240	0.303	0.287	0.232	0.313
0.075	CoV	0.308	0.292	0.369	0.336	0.309	0.408	0.335	0.303	0.435
	Max.	1.34	1.23	1.22	1.18	1.02	1.10	1.19	1.02	1.11
	Min.	0.363	0.363	0.363	0.232	0.232	0.232	0.226	0.225	0.192
	Mean	0.939	0.836	0.824	0.890	0.788	0.765	0.878	0.776	0.735
	SD	0.282	0.230	0.291	0.296	0.232	0.302	0.293	0.227	0.313
0.1	CoV	0.300	0.276	0.353	0.332	0.295	0.395	0.334	0.292	0.426
	Max.	1.37	1.26	1.24	1.25	1.04	1.13	1.26	1.02	1.13
	Min.	0.435	0.435	0.426	0.280	0.280	0.280	0.262	0.261	0.222
	Mean	1.06	0.921	0.951	0.995	0.853	0.883	0.974	0.833	0.854
	SD	0.306	0.217	0.299	0.324	0.206	0.321	0.334	0.209	0.344
0.25	CoV	0.288	0.236	0.315	0.326	0.242	0.363	0.342	0.251	0.403
	Max.	1.57	1.39	1.34	1.57	1.18	1.28	1.58	1.06	1.29
	Min.	0.499	0.495	0.401	0.492	0.488	0.397	0.453	0.453	0.395

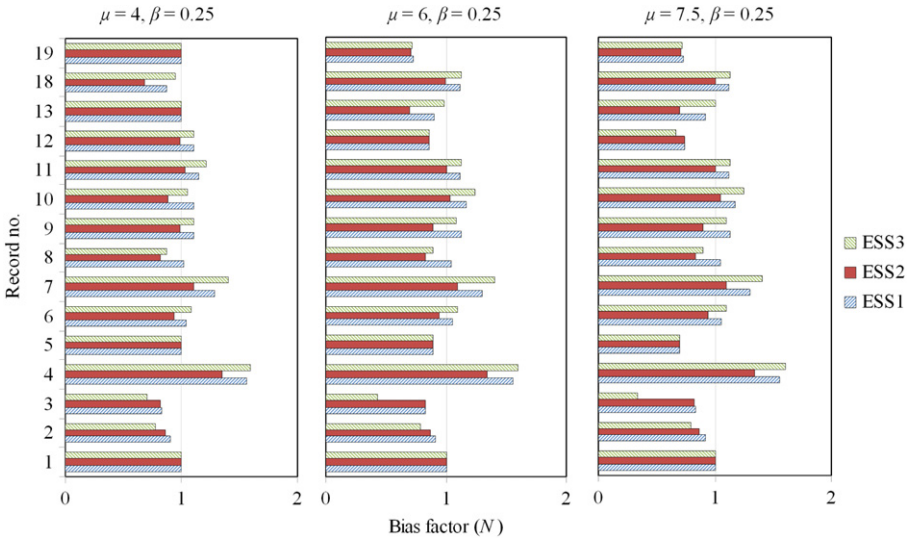

Fig. 5. Bar charts for the bias factor (N) for the nine-storey frame, for $\beta = 0.25$.

Table 11
Bias factor (N) values for all ESS for the three-storey building, with $\beta = 0.25$.

Record No.	$\mu = 4.0$			$\mu = 6.0$			$\mu = 7.5$		
	ESS1	ESS2	ESS3	ESS1	ESS2	ESS3	ESS1	ESS2	ESS3
1	1.00	1.00	1.00	1.00	1.00	1.00	1.00	1.00	1.00
2	1.00	1.00	1.00	1.00	1.00	1.00	0.993	0.887	0.807
3	1.00	1.00	1.00	0.859	0.859	0.859	0.837	0.737	0.666
4	1.00	1.00	1.00	0.876	0.778	0.772	0.876	0.779	0.597
5	1.00	1.00	1.00	1.00	1.00	1.00	0.816	0.816	0.816
6	1.00	1.00	1.00	1.00	1.00	1.00	1.04	1.01	0.988
7	1.00	1.00	1.00	1.00	1.00	1.00	0.964	0.964	0.964
8	1.00	1.00	1.00	1.00	1.00	1.06	1.26	1.00	1.38
9	1.00	1.00	1.00	1.00	1.00	1.00	1.00	1.00	1.00
10	1.00	1.00	1.00	1.00	1.00	1.00	1.06	1.03	1.00
11	1.00	1.00	1.00	1.00	1.00	1.00	0.810	0.810	0.810
12	0.879	0.777	0.777	0.784	0.668	0.661	0.865	0.666	0.667
13	1.00	1.00	1.00	1.00	1.00	1.43	1.03	0.923	1.56
14	1.00	1.00	1.00	1.24	1.22	1.00	1.60	1.58	1.00
15	1.00	1.00	1.00	1.03	0.984	1.27	1.03	0.983	1.28
16	1.16	1.13	0.888	1.16	1.13	0.800	1.43	1.40	1.00
17	1.24	1.19	0.673	1.23	1.17	0.556	1.23	1.17	0.560

drift ratio (Δ_{mi}) for the ith storey is defined as the maximum value of the ith interstorey drift ratio ($\Delta_i(t)$) during the earthquake:

$$\Delta_i(t) = \frac{D_i(t) - D_{i-1}(t)}{h_i} \tag{16}$$

where D_i is the ith-floor displacement and h_i is the ith-storey height. Δ_{mi} is often preferred over the maximum roof displacement (D_m) because it can indicate the occurrence or non-occurrence of the soft-storey mechanism in one storey of a building frame. For many old and poorly detailed structures, it is quite likely that the drift demands are not close to uniform over all the storeys and there may exist a significant concentration of this demand at one storey relative to all others. The definition of D_{PA} is modified in this section in order to reflect the maximum interstorey drift demand (with respect to capacity). D_{PA} based on the interstorey drift ratio is defined as

$$D_{\mathrm{PA}} = \left(\frac{\Delta_{mi} - \Delta_{yi}}{\Delta_{ui} - \Delta_{yi}}\right)\Bigg|_{\mathrm{max}i} + \frac{\beta}{V_y D_u}\int \mathrm{d}E_h. \tag{17}$$

It should be noted that the difference between Eqs. (14) and (17) is only in the ductility part of the D_{PA}. Even for the interstorey drift ratio-based definition of D_{PA}, the cumulative energy part is calculated from the hysteretic energy demand on the whole structure and it is normalized by the yield base shear (V_y) and the monotonic roof displacement capacity (D_u). For the ductility part of this D_{PA}, the maximum demand to capacity ratio among all storeys is used. β, here, obviously needs a different calibration from the β in Eq. (14). Δ_{yi} is the yield value corresponding to the ith interstorey drift ratio. Δ_{yi} is obtained from a storey shear (V_i) versus interstorey drift ratio (Δ_i) "pushover" plot based on the NSPA, similar to Fig. 1 for D_y. The monotonic interstorey drift ratio capacity, Δ_{ui}, is defined on the basis of an assumed ductility capacity (μ) at the storey level, which is assumed to be the same for all storeys:

$$\Delta_{ui} = \mu\Delta_{yi}. \tag{18}$$

This ductility capacity is usually not the same as the roof displacement-based ductility capacity used in Eq. (14) for D_u. For case studies based on this new definition of D_{PA}, however, we use the same μ values as were considered for the other two sets of case studies presented in the two previous sections.

The basis of the equivalent schemes remains the same for this third set of case studies, although the ESS get slightly modified, in order to account for D_m getting replaced by Δ_{mi}. For ESS1 and ESS3, the peak interstorey drift demand for the ith storey is obtained by multiplying the displacement demand (D_m) with a factor based on the assumed mode shape/displacement profile:

$$\Delta_{mi} = \left[\frac{(\phi_i - \phi_{i-1})/h_i}{\phi_r}\right] D_m \tag{19}$$

Table 12
Bias (N) statistics summary for the three-storey building with varying β values, for D_{PA} based on the maximum interstorey drift.

β		$\mu = 4.0$			$\mu = 6.0$			$\mu = 7.5$		
		ESS1	ESS2	ESS3	ESS1	ESS2	ESS3	ESS1	ESS2	ESS3
	Mean	1.04	1.01	0.928	1.05	0.976	0.817	1.12	1.04	0.767
	SD	0.115	0.107	0.151	0.228	0.227	0.202	0.349	0.345	0.259
0.01	CoV	0.111	0.106	0.162	0.217	0.233	0.247	0.311	0.331	0.338
	Max.	1.42	1.33	1.00	1.52	1.49	1.10	1.97	1.94	1.24
	Min.	0.901	0.788	0.562	0.627	0.622	0.468	0.627	0.622	0.418
	Mean	1.04	1.01	0.932	1.05	0.970	0.830	1.11	1.04	0.780
	SD	0.110	0.103	0.150	0.217	0.218	0.201	0.340	0.336	0.261
0.025	CoV	0.103	0.102	0.158	0.207	0.224	0.242	0.305	0.324	0.335
	Max.	1.40	1.32	1.00	1.49	1.47	1.13	1.94	1.91	1.28
	Min.	0.947	0.782	0.568	0.636	0.630	0.474	0.636	0.631	0.443
	Mean	1.03	1.01	0.938	1.04	0.969	0.853	1.08	0.996	0.785
	SD	0.100	0.100	0.142	0.201	0.205	0.202	0.313	0.326	0.236
0.05	CoV	0.0968	0.0988	0.151	0.193	0.212	0.237	0.289	0.327	0.301
	Max.	1.38	1.30	1.00	1.46	1.44	1.18	1.90	1.87	1.18
	Min.	0.982	0.771	0.580	0.648	0.643	0.483	0.649	0.644	0.484
	Mean	1.03	1.01	0.941	1.06	0.971	0.875	1.07	1.01	0.807
	SD	0.0960	0.0980	0.136	0.218	0.192	0.204	0.300	0.299	0.238
0.075	CoV	0.0930	0.0970	0.144	0.206	0.198	0.233	0.280	0.296	0.295
	Max.	1.36	1.28	1.00	1.53	1.41	1.23	1.85	1.83	1.24
	Min.	0.964	0.762	0.592	0.677	0.677	0.493	0.661	0.656	0.494
	Mean	1.03	1.01	0.9441	1.03	0.974	0.893	1.07	0.993	0.828
	SD	0.0920	0.0968	0.130	0.169	0.179	0.205	0.289	0.296	0.241
0.1	CoV	0.0896	0.0959	0.137	0.163	0.184	0.229	0.271	0.298	0.291
	Max.	1.34	1.27	1.00	1.40	1.38	1.28	1.81	1.79	1.29
	Min.	0.949	0.754	0.603	0.729	0.701	0.502	0.671	0.666	0.503
	Mean	1.02	1.01	0.961	1.01	0.989	0.965	1.05	0.986	0.947
	SD	0.0770	0.0796	0.0946	0.116	0.131	0.204	0.218	0.229	0.271
0.25	CoV	0.0757	0.0791	0.0985	0.115	0.132	0.212	0.208	0.233	0.287
	Max.	1.24	1.19	1.00	1.24	1.22	1.43	1.60	1.58	1.56
	Min.	0.879	0.777	0.673	0.784	0.668	0.556	0.810	0.666	0.560

where ϕ_i is the ith-floor element of the mode shape/displacement vector, and ϕ_r is the element corresponding to the roof for the same vector. For ESS2, the peak interstorey drift demand is obtained from an SRSS combination of individual modal demands after applying a proper ground motion scaling factor for each mode:

$$\Delta_{mi} = \sqrt{\sum_n \left(\left[\frac{(\phi_{in} - \phi_{i-1,n})/h_i}{\phi_{rn}} \right] D_{mn} \right)^2} \tag{20}$$

where the subscript n denotes an nth modal parameter. Like in the previous case studies, the first two modes are used for ESS2 for the three-storey frame and the first five modes are combined for ESS2 for the nine- and twenty-storey frames. Δ_{mi} from Eqs. (19) (or (20)) is used in Eq. (17) to obtain D_{PA-ES}. The Δ_{yi} and Δ_{ui} values for all ESS are based on the NSPA of the MDOF model.

Case studies for this definition of D_{PA} are based on the same three-, nine-, and twenty-storey framed structures, with $\mu = 4$, 6, and 7.5, and β ranging from 0.01 to 0.25, as in Section 5. Bias factor (N) statistics are obtained for the same set of scaled records as were mentioned in the previous two case studies. A sample of what the bias values are for individual earthquakes is presented in Table 11 for the three-storey frame and $\beta = 0.25$ for all the ESS and all μ values. The summaries of the bias statistics for D_{PA} based on the maximum interstorey drift ratio are presented in Tables 12–14, for all the β values considered. It is observed that for the three-storey frame, all three ESS provide very good estimations of the actual damage index (that is, D_{PA-M}). The mean bias values are close to 1.0 and the coefficients of variation are low. This is expected as for the three-storey frame, the first mode dominates the vibration and there is not a significant difference between the three ESS for this frame. In addition, the maximum interstorey drift ratio is very close to the maximum global drift ratio, which is defined as the ratio of the maximum roof displacement to the height of the frame. On the basis of the case study frame and selected records, the ESS are as effective in estimating the damage index based on the maximum interstorey drift ratio as they are for the global D_{PA} used in the previous case studies. Like for those two case studies, it is observed that ESS1 and ESS2 provide slightly better estimates than ESS3. For the nine- and twenty-storey frames, however, there are significant differences among the statistics for the three different ESS. From a mean bias perspective, ESS2 provides the best results. The mean bias values for this ESS are in the same range for the three-, nine- and twenty-storey frames. ESS1 shows an underestimation of the actual D_{PA}, while ESS3 shows an overestimation, in all cases for the nine- and twenty-storey frames. However, ESS3 gives better estimates compared to ESS1. ESS2 and ESS3 give low CoV values as well. Sample plots are provided in Figs. 6–8, for $\beta = 0.025$, for all the frames.

These results indicate that the inclusion of the higher mode effects (in ESS2) pay off for D_{PA} based on the maximum interstorey drift ratio, particularly for the high-rises. In fact, ESS2 estimates are better for the D_{PA} based on the maximum interstorey drift compared to the estimates for D_{PA} based on the maximum roof displacement. This should be evident from a comparison of the mean and standard deviation/CoV of bias between Tables 9, 10, 13 and 14. For the twenty-storey frame, considering all the μ and β values, the mean bias varies in a narrow range of 0.995–1.07, and the maximum CoV value is only 0.278 (Table 14). This implies that ESS2 is very effective in estimating the D_{PA} demands for high-rises, even when the damage index is based on a storey-level behaviour. Looking into the details of the D_{PA} estimates, one can see why the ESS2 estimates are better for this case study. The primary reason for this is that for many of the eleven scaled records used for the twenty-storey building, D_{PA} based on the maximum interstorey drift reaches (or would exceed, if it was not upper bounded) 1.0, signifying collapse. For such earthquakes, ESS2 (like ESS3, most of the time) accurately predicts the D_{PA} demand ($D_{PA-M} = D_{PA-ES} = 1.0$). This reduces the CoV and brings the mean bias very close

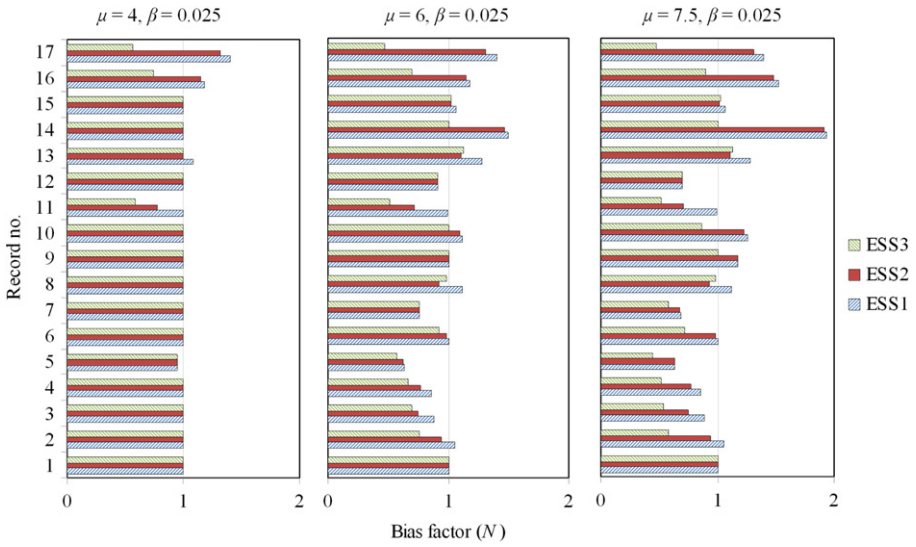

Fig. 6. Sample bar charts for the bias (N) in estimating D_{PA} based on the maximum interstorey drift ratio for the three-storey frame.

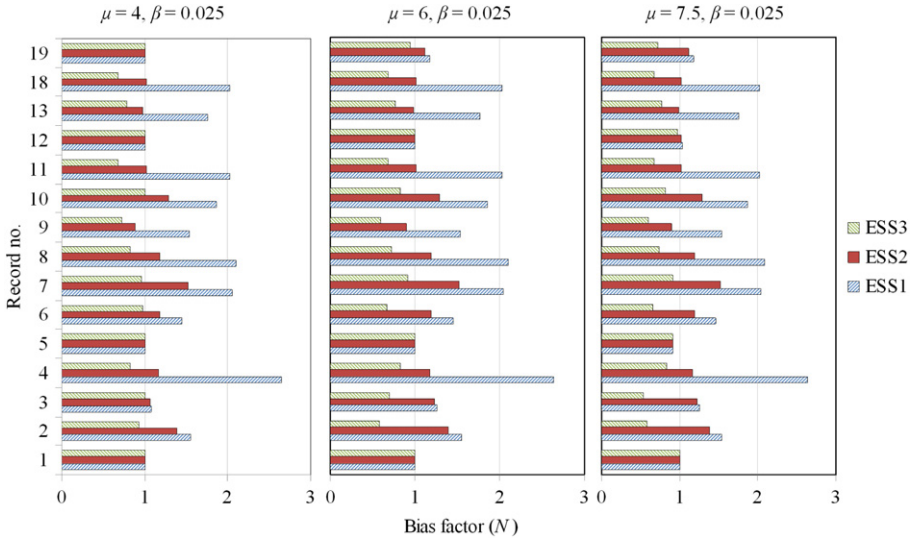

Fig. 7. Sample bar charts for the bias (N) in estimating D_{PA} based on the maximum interstorey drift ratio for the nine-storey frame.

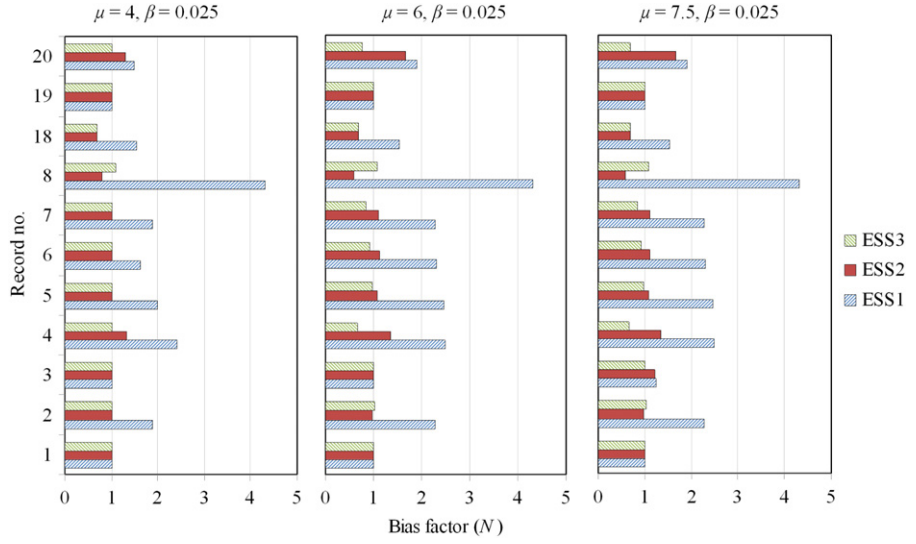

Fig. 8. Sample bar charts for the bias (N) in estimating D_{PA} based on the maximum interstorey drift ratio for the twenty-storey frame.

Table 13
Bias (N) statistics summary for the nine-storey building with varying β values, for D_{PA} based on the maximum interstorey drift.

β		$\mu = 4.0$			$\mu = 6.0$			$\mu = 7.5$		
		ESS1	ESS2	ESS3	ESS1	ESS2	ESS3	ESS1	ESS2	ESS3
	Mean	1.61	1.12	0.885	1.63	1.13	0.787	1.63	1.13	0.753
	SD	0.520	0.178	0.129	0.497	0.181	0.151	0.504	0.182	0.145
0.01	CoV	0.323	0.159	0.146	0.305	0.160	0.192	0.310	0.161	0.193
	Max.	2.66	1.53	1.00	2.66	1.53	1.00	2.66	1.53	1.00
	Min.	1.00	0.889	0.670	1.00	0.889	0.575	0.900	0.889	0.531
	Mean	1.61	1.11	0.892	1.63	1.13	0.793	1.63	1.13	0.760
	SD	0.517	0.174	0.127	0.492	0.172	0.149	0.497	0.177	0.145
0.025	CoV	0.322	0.156	0.142	0.302	0.152	0.188	0.306	0.156	0.190
	Max.	2.65	1.52	1.00	2.64	1.52	1.00	2.64	1.52	1.00
	Min.	1.00	0.893	0.674	1.00	0.894	0.586	0.915	0.894	0.535
	Mean	1.60	1.11	0.902	1.63	1.13	0.803	1.62	1.13	0.772
	SD	0.510	0.167	0.123	0.483	0.166	0.147	0.486	0.168	0.144
0.05	CoV	0.319	0.150	0.136	0.297	0.146	0.183	0.299	0.149	0.187
	Max.	2.62	1.50	1.00	2.61	1.50	1.00	2.61	1.50	1.00
	Min.	1.00	0.900	0.681	1.00	0.901	0.595	0.939	0.902	0.542
	Mean	1.59	1.11	0.911	1.63	1.13	0.814	1.62	1.13	0.773
	SD	0.503	0.158	0.119	0.475	0.164	0.143	0.475	0.165	0.163
0.075	CoV	0.317	0.143	0.131	0.292	0.145	0.176	0.292	0.146	0.211
	Max.	2.59	1.47	1.00	2.58	1.48	1.00	2.58	1.48	1.00
	Min.	1.00	0.906	0.687	1.00	0.908	0.623	0.963	0.909	0.452
	Mean	1.58	1.10	0.918	1.62	1.13	0.820	1.62	1.12	0.796
	SD	0.495	0.145	0.114	0.470	0.156	0.141	0.466	0.134	0.144
0.1	CoV	0.314	0.132	0.124	0.290	0.138	0.172	0.287	0.119	0.181
	Max.	2.57	1.42	1.00	2.56	1.46	1.00	2.55	1.34	1.00
	Min.	1.00	0.912	0.694	1.00	0.914	0.615	0.988	0.915	0.555
	Mean	1.50	1.06	0.950	1.60	1.12	0.868	1.61	1.09	0.850
	SD	0.469	0.0890	0.0947	0.444	0.144	0.115	0.429	0.220	0.134
0.25	CoV	0.312	0.0836	0.100	0.278	0.128	0.132	0.266	0.201	0.157
	Max.	2.43	1.29	1.00	2.41	1.38	1.00	2.40	1.38	1.01
	Min.	1.00	1.00	0.732	1.00	0.944	0.723	1.00	0.470	0.595

Table 14
Bias (N) statistics summary for the twenty-storey building with varying β values, for D_{PA} based on the maximum interstorey drift.

β		$\mu = 4.0$			$\mu = 6.0$			$\mu = 7.5$		
		ESS1	ESS2	ESS3	ESS1	ESS2	ESS3	ESS1	ESS2	ESS3
	Mean	1.85	1.01	0.979	2.06	1.05	0.903	2.08	1.07	0.897
	SD	0.946	0.189	0.101	0.966	0.292	0.145	0.941	0.297	0.152
0.01	CoV	0.512	0.186	0.103	0.469	0.278	0.161	0.452	0.276	0.170
	Max.	4.32	1.33	1.08	4.32	1.67	1.08	4.32	1.67	1.08
	Min.	1.00	0.684	0.683	1.00	0.584	0.658	1.00	0.584	0.658
	Mean	1.83	1.01	0.979	2.05	1.05	0.905	2.07	1.07	0.899
	SD	0.940	0.185	0.100	0.961	0.289	0.145	0.936	0.293	0.153
0.025	CoV	0.513	0.183	0.102	0.469	0.275	0.161	0.452	0.273	0.170
	Max.	4.31	1.32	1.09	4.31	1.66	1.09	4.31	1.66	1.09
	Min.	1.00	0.686	0.687	1.00	0.586	0.660	1.00	0.586	0.660
	Mean	1.81	1.009	0.981	2.03	1.05	0.908	2.05	1.07	0.902
	SD	0.931	0.178	0.0994	0.951	0.284	0.146	0.928	0.287	0.154
0.05	CoV	0.515	0.177	0.101	0.467	0.270	0.161	0.452	0.268	0.171
	Max.	4.29	1.30	1.09	4.29	1.64	1.10	4.29	1.64	1.10
	Min.	1.00	0.689	0.693	1.00	0.589	0.663	1.00	0.589	0.663
	Mean	1.79	1.00	0.982	2.02	1.05	0.912	2.04	1.07	0.906
	SD	0.923	0.172	0.0986	0.942	0.279	0.147	0.920	0.281	0.156
0.075	CoV	0.517	0.171	0.100	0.467	0.266	0.161	0.451	0.264	0.172
	Max.	4.27	1.29	1.10	4.26	1.62	1.11	4.26	1.62	1.11
	Min.	1.00	0.692	0.700	1.00	0.592	0.666	1.00	0.593	0.666
	Mean	1.76	1.01	0.983	2.01	1.05	0.916	2.02	1.06	0.909
	SD	0.916	0.166	0.0979	0.934	0.274	0.148	0.913	0.275	0.157
0.1	CoV	0.519	0.165	0.100	0.466	0.262	0.161	0.451	0.259	0.173
	Max.	4.25	1.27	1.11	4.24	1.60	1.12	4.24	1.60	1.12
	Min.	1.00	0.694	0.706	1.00	0.595	0.668	1.00	0.596	0.669
	Mean	1.65	0.995	0.991	1.93	1.04	0.936	1.94	1.05	0.929
	SD	0.883	0.133	0.0953	0.892	0.247	0.154	0.876	0.246	0.168
0.25	CoV	0.536	0.134	0.0962	0.461	0.238	0.164	0.451	0.235	0.181
	Max.	4.14	1.19	1.16	4.13	1.50	1.17	4.12	1.50	1.17
	Min.	1.00	0.709	0.743	1.00	0.613	0.684	1.00	0.614	0.665

Table 15
Bias (N) statistics for ESS2 for the twenty-storey building considering $\mu = 10.0$, for D_{PA} based on the maximum interstorey drift.

	β					
	0.01	0.025	0.05	0.075	0.1	0.25
Mean	1.11	1.10	1.10	1.09	1.08	1.06
SD	0.307	0.302	0.294	0.287	0.282	0.252
CoV	0.277	0.274	0.268	0.263	0.262	0.238
Max.	1.67	1.66	1.64	1.62	1.60	1.49
Min.	0.584	0.586	0.590	0.593	0.596	0.615

to the ideal value. As the ductility capacity increases from 4.0 to 7.5, the spread becomes greater as the lesser number of records leads to $D_{PA} = 1.0$. Table 15 shows how the quality of estimation for ESS2 for $\beta = 0.25$ deteriorates further for $\mu = 10.0$. The interstorey drift ductility capacity of 10.0 is based on an average Δ_{yi} of 0.64% for the twenty storeys and an interstorey drift capacity of 0.06 for high-rise ordinary moment frames as per FEMA-350 [49]. The numbers of records for which $D_{PA} = 1.0$ are 8, 3, 2, and 1, respectively, for $\mu = 4.0, 6.0, 7.5$, and 10.0. However, even for $\mu = 10.0$, where only one out of eleven records has $D_{PA} = 1.0$, the estimates are very good. Therefore, it can be concluded that ESS2 provides very good estimates for D_{PA} based on the maximum interstorey drift for the twenty-storey structure.

7. Concluding remarks

This paper proposes various equivalent systems for estimating the Park–Ang damage index for building frame structures, and measures the effectiveness of these equivalent system schemes through a detailed statistical study. Two different definitions of the damage index are considered: based on the maximum roof displacement and the maximum interstorey drift demands. The case studies include low-, mid- and high-rise frames, three different values of the ductility capacity and five different β values ranging from 0.01 to 0.25. On the basis of the summary statistics, the following can be concluded for the equivalent system schemes proposed.

- *ESS1*: This equivalent system is very easy to construct as it is based on a single pushover analysis using the fundamental mode shape. It provides the best estimates among all the ESS for D_{PA} based on the maximum roof displacement, across low- to high-rise frames, and different μ and β values considered. However, ESS1 is found to provide the poorest estimates for D_{PA} based on the maximum interstorey drift (except for the low-rise building, where it can be used).
- *ESS2*: This equivalent system is not very easy to construct as it considers multiple single-degree-of-freedom systems on the basis of multiple pushover analyses. It cannot be recommended for everyday design/evaluation purposes, as it involves a lot of computation. However, this ESS provides the best estimates for D_{PA} based on the maximum interstorey drift and these are excellent estimates considering performances of any kind of equivalent system. These estimates are also significantly better than those of the other two ESS. The first five modes are found adequate for inclusion in ESS2 for these estimates (considering just the first three modes is sufficient, mostly). ESS2 is not recommended for D_{PA} based on the maximum roof displacement as ESS1 is an easier and better solution for that.
- *ESS3*: ESS3 can be constructed easily since it is based on a single pushover analysis using the familiar IBC 2006 recommended distribution. Generally, this ESS never gives the best estimates among the three ESS for any case. However, it can be recommended for estimating D_{PA} based on the maximum interstorey drift for high- and mid-rise frames, where ESS1 yields very bad estimates and the user may find ESS2 to be too computation-heavy to use.

These recommendations can be used to select the proper ESS for estimating D_{PA} for both performance evaluation and design purposes. The primary advantage of using these approximate schemes is that these can use response spectra to estimate the demand on the structure. The approximate procedures also reduce computation by a significant margin compared to the NLRHA of MDOF systems for finding the actual D_{PA}, although not to the same extent for all the ESS proposed here. The mean and CoV of the bias can be used to statistically correlate the actual and the approximate damage indices. A better statistics can be generated following the method used here for a wider variety of frames. The presented bias statistics may be sensitive to the records selected. It would be better if a very large set of ground records were used to generate these statistics and these generalized statistics can be directly adopted for everyday use. Alternatively, similar statistics can be generated specifically for earthquakes of a certain type (for example, near-field earthquakes) only and/or for ground characteristics of a certain type. The bias statistics can also be presented from the perspective of the fundamental period of the structure instead of relating it to the building height. This research should be extended to degrading systems such as RC frames and shear wall structures to make it more general. Future extensions should also focus on even further localized definitions of the Park–Ang damage index.

Acknowledgements

The authors would like to thank Charugalla J. P. Sreeram, graduate student in the Department of Civil Engineering, Indian Institute of Technology Bombay, for his help with the data analysis.

References

[1] SEAOC. Vision 2000: performance based seismic engineering of buildings. Sacramento (CA, USA): Structural Engineers Association of California; 1995.
[2] Ghobarah A. Performance-based design in earthquake engineering: state of development. Eng Struct 2001;23(8):878–84.
[3] Qi X, Moehle JP. Displacement design approach to reinforced concrete structures subjected to earthquakes. Tech. rep. Berkeley (CA, USA): University of California; 1991.
[4] Collins KR, Wen Y-K, Foutch DA. Dual-level seismic design: a reliability-based methodology. Earthquake Eng Struct Dyn 1996;25(12):1433–67.
[5] Priestley MJN, Calvi GM, Kowalsky MJ. Displacement based seismic design of structures. Pavia: IUSS Press; 2007.
[6] Chao S-H, Goel SC, Lee S-S. A seismic design lateral force distribution based on inelastic state of structures. Earthq Spectra 2007;23(3):547–69.
[7] Ghosh S, Das A, Adam F. Design of steel plate shear walls considering inelastic drift demand. J Constr Steel Res 2009;65(7):1431–7.
[8] Zahrah TF, Hall WJ. Earthquake energy absorption in SDOF structures. J Struct Eng, ASCE 1984;110(8):1757–72.
[9] Fajfar P. Equivalent ductility factors, taking into account low-cycle fatigue. Earthquake Eng Struct Dyn 1992;21(10):837–48.
[10] Ghosh S, Collins KR. Merging energy-based design criteria and reliability-based methods: exploring a new concept. Earthquake Eng Struct Dyn 2006; 35(13):1677–98.
[11] Park Y-J, Ang AH-S. Mechanistic seismic damage model for reinforced concrete. J Struct Eng, ASCE 1985;111(4):722–39.
[12] Datta D, Ghosh S. Uniform hazard spectra based on Park–Ang damage index. J Earthq Tsunami 2008;2(3):241–58.
[13] Banon H, Biggs JM, Irvine HM. Seismic damage in reinforced concrete frames. J Struct Eng, ASCE 1981;107(9):1713–29.
[14] Roufaiel MSL, Meyer C. Analytical modelling of hysteretic behaviour of R/C frames. J Struct Eng, ASCE 1987;113(3):429–57.
[15] Stephens JE, Yao JTP. Damage assessment using response measurement. J Struct Eng, ASCE 1987;113(4):787–801.
[16] Wang ML, Shah SP. Reinforced concrete hysteresis model based in the damage concept. Earthquake Eng Struct Dyn 1987;15(8):993–1003.
[17] Powell GH, Allahabadi R. Seismic damage prediction by deterministic methods: concepts and procedures. Earthquake Eng Struct Dyn 1988;16(5): 719–34.
[18] Jeong GD, Iwan WD. Effect of earthquake duration on damage of structures. Earthquake Eng Struct Dyn 1988;16(8):1201–11.
[19] Chung YS, Meyer C, Shinozuka M. Modeling of concrete damage. ACI Struct J 1989;86(3):259–71.
[20] Hwang TH, Scribner CF. R/C member cyclic response during various loadings. J Struct Eng, ASCE 1984;110(3):477–89.

[21] Kunnath SK, Reinhorn AM, Lobo RF. IDARC version 3.0: a program for the inelastic damage analysis of reinforced concrete structures. Report no. NCEER-92-0022. Buffalo (NY, USA): National Center for Earthquake Engineering and Research, SUNY; 1992.
[22] Carr AJ, Tabuchi M. The structural ductility and the damage index for reinforced concrete structure under seismic excitation, in: 2nd European conference on structural dynamics. vol. 1. 1993. p. 169–76.
[23] Cosenza E, Manfredi G, Ramasco R. The use of damage functionals in earthquake engineering: a comparison between different models. Earthquake Eng Struct Dyn 1993;22(10):855–68.
[24] Kunnath SK, Jenne C. Seismic damage assessment of inelastic rc structures. In: 5th US national conference on earthquake engineering. vol. 1. 1994. p. 55–64.
[25] Ghobarah A, Abou-Elfath H, Biddah A. Response-based damage assessment of structures. Earthquake Eng Struct Dyn 1999;28(1):79–104.
[26] Williams MS, Sexsmith RG. Seismic damage indices for concrete structures: a state-of-the-art review. Earthq Spectra 1995;11(2):319–49.
[27] Park YJ, Ang AH, Wen YK. Damage-limiting aseismic design of buildings. Earthq Spectra 1987;3(1):1–26.
[28] van de Lindt JW. Damage-based seismic reliability concept for woodframe structures. J Struct Eng, ASCE 2005;131(4):668–75.
[29] Roth DH, Sozen MA. A SDOF model to study nonlinear dynamic response of large- and small-scale R/C test structures. Structural research series report no. 512. Urbana (IL, USA): University of Illinois; 1983.
[30] Lee DG. Accurate and simplified models for seismic response prediction of steel frame structures. Ph.D. thesis. Palo Alto (CA, USA): Stanford University; 1984.
[31] Miranda E. Seismic evaluation and upgrading of existing buildings. Ph.D. thesis. Berkeley (CA, USA): University of California; 1991.
[32] Han SW, Wen Y-K. Method of reliability-based seismic design. I: equivalent nonlinear systems. J Struct Eng, ASCE 1997;123(3):256–63.
[33] Chopra AK, Goel RK. A modal pushover analysis procedure for estimating seismic demands for buildings. Earthquake Eng Struct Dyn 2002;31(3):561–82.
[34] Chopra AK, Goel RK. A modal pushover analysis procedure to estimate seismic demands for unsymmetric-plan buildings. Earthquake Eng Struct Dyn 2004;33(8):903–27.
[35] Lin J-L, Tsai K-C. Simplified seismic analysis of asymmetric building systems. Earthquake Eng Struct Dyn 2007;36(4):459–79.
[36] Makarios TK. Equivalent non-linear single-degree-of-freedom system of spatial asymmetric multi-storey buildings in pushover procedure: theory and applications. Struct Des Tall Special Build 2009;18(7):729–63.
[37] Makarios TK. Optimum definition of equivalent non-linear SDF system in pushover procedure of multistory R/C frames. Eng Struct 2005;27(5):814–25.
[38] Fajfar P, Gašperšič P. The N2 method for the seismic damage analysis of RC buildings. Earthquake Eng Struct Dyn 1996;25(1):31–46.
[39] Chou C-C, Uang C-M. A procedure for evaluating seismic energy demand of framed structures. Earthquake Eng Struct Dyn 2003;32(2):229–44.
[40] Prasanth T, Ghosh S, Collins KR. Estimation of hysteretic energy demand using concepts of modal pushover analysis. Earthquake Eng Struct Dyn 2008;37(6):975–90.
[41] Rathore M, Chowdhury ARoy, Ghosh S. Approximate methods for estimating hysteretic energy demand on plan-asymmetric buildings. Journal of Earthquake Engineering 2011;15(1):99–123.
[42] ICC. International building code (IBC). Whittier (CA, USA): International Code Council; 2006.
[43] Chase JG, Barroso LR, Hunt S. The impact of total acceleration control for semi-active earthquake hazard mitigation. Eng Struct 2004;26(2):201–9.
[44] Gupta A, Krawinkler H. Seismic demands for performance evaluation of steel moment resisting frame structures. John A. Blume earthquake engineering center report no. 132. Stanford (USA): Department of Civil Engineering, Stanford University; 1999.
[45] Prakash V, Powell GH, Campbell S. DRAIN-2DX. Base program description and user guide: version 1.10. Report no. UCB/SEMM-93/17. Berkeley (CA, USA): University of California; 1993.
[46] Park YJ, Ang AH-S, Wen Y-K. Seismic damage analysis and damage-limiting design of R/C buildings. Structural research series report no. 516. Urbana (IL, USA): University of Illinois; 1984.
[47] Chai YH, Romstad KM, Bird SM. Energy-based linear damage model for high-intensity seismic loading. J Struct Eng, ASCE 1995;121(5):857–64.
[48] Alarcón E, Recuero A, Perera R, López C, Gutiérrez JP, De Diego A, et al. A repairability index for reinforced concrete members based on fracture mechanics. Eng Struct 2001;23(6):687–97.
[49] FEMA. Recommended seismic design criteria for new steel moment-frame buildings (FEMA-350). Washington (DC, USA): Federal Emergency Management Agency; 2000.